Tectonics

RESEARCH ARTICLE
10.1029/2017TC004941

Key Points:
- The 2016–2017 seismic sequence is related to the wide NNE-SSW sinistral fault zone located in the central part of the Alboran Sea
- Epicentral sea bottom deformations include mass transport deposits and recent faults
- Seismicity and sea bottom deformations are located west of the main Al Idrisi Fault, supporting the westward widening of the fault zone

Correspondence to:
J. Galindo-Zaldivar,
jgalindo@ugr.es

Citation:
Galindo-Zaldivar, J., Ercilla, G., Estrada, F., Catalán, M., d'Acremont, E., Azzouz, O., et al (2018). Imaging the growth of recent faults: The case of 2016–2017 seismic sequence sea bottom deformation in the Alboran Sea (western Mediterranean). *Tectonics*, *37*, 2513–2530. https://doi.org/10.1029/2017TC004941

Received 24 DEC 2017
Accepted 10 JUL 2018
Accepted article online 16 JUL 2018
Published online 12 AUG 2018

Imaging the Growth of Recent Faults: The Case of 2016–2017 Seismic Sequence Sea Bottom Deformation in the Alboran Sea (Western Mediterranean)

J. Galindo-Zaldivar[1,2], G. Ercilla[3], F. Estrada[3], M. Catalán[4], E. d'Acremont[5], O. Azzouz[6], D. Casas[7], M. Chourak[6], J. T. Vazquez[8], A. Chalouan[9], C. Sanz de Galdeano[1], M. Benmakhlouf[10], C. Gorini[5], B. Alonso[3], D. Palomino[8], J. A. Rengel[11], and A. J. Gil[12,13]

[1]Instituto Andaluz de Ciencias de la Tierra, CSIC-UGR, Granada, Spain, [2]Departamento de Geodinámica, Universidad de Granada, Granada, Spain, [3]Institut de Ciències del Mar, GMC, ICM-CSIC, Barcelona, Spain, [4]Real Instituto y Observatorio de la Armada, San Fernando, Spain, [5]Sorbonne Universités, UPMC Université Paris 06 UMR 7193, ISTeP, Paris, France, [6]Université Mohammed Premier, Oujda, Morocco, [7]Instituto Geológico y Minero de España, Madrid, Spain, [8]Instituto Español de Oceanografía, Fuengirola, Spain, [9]Faculté des Sciences, Université Mohammed V-Agdal, Rabat, Morocco, [10]Faculté des Sciences, Université Abdelmalek Essaadi, Tetouan, Morocco, [11]Instituto Hidrográfico de la Marina IHM, Cádiz, Spain, [12]Departamento Ingenieria Cartográfica, Geodesia y Fotogrametría, Universidad de Jaén, Jaén, Spain, [13]CEACTierra, Universidad de Jaén, Jaén, Spain

Abstract The Eurasian-African NW-SE oblique plate convergence produces shortening and orthogonal extension in the Alboran Sea Basin (westernmost Mediterranean), located between the Betic and Rif Cordilleras. A NNE-SSW broadband of deformation and seismicity affects the Alboran central part. After the 1993–1994 and 2004 seismic series, an earthquake sequence struck mainly its southern sector in 2016–2017 (main event M_w = 6.3, 25 January 2016). The near-surface deformation is investigated using seismic profiles, multibeam bathymetry, gravity and seismicity data. Epicenters can be grouped into two main alignments. The northern WSW-ENE alignment has reverse earthquake focal mechanisms, and in its epicentral region recent mass transport deposits occur. The southern alignment consists of a NNE-SSW vertical sinistral deformation zone, with early epicenters of higher-magnitude earthquakes located along a narrow band 5 to 10-km offset westward of the Al Idrisi Fault. Here near-surface deformation includes active NW-SE vertical and normal faults, unmapped until now. Later, epicenters spread eastward, reaching the Al Idrisi Fault, characterized by discontinuous active NNE-SSW vertical fractures. Seismicity and tectonic structures suggest a westward propagation of deformation and the growth at depth of incipient faults, comprising a NNE-SSW sinistral fault zone in depth that is connected upward with NW-SE vertical and normal faults. This recent fault zone is segmented and responsible for the seismicity in 1993–1994 in the coastal area, in 2004 onshore, and in 2016–2017 offshore. Insights for seismic hazard assessment point to the growth of recent faults that could produce potentially higher magnitude earthquakes than the already formed faults.

1. Introduction

Continuous plate motion has led to the activity of tectonic structures developed along plate boundaries, including faults with related seismicity. Seismic or creep behavior of a fault is constrained by the rheology of the deformed rocks (Sibson, 1977). Brittle deformation is generally accommodated by previous fractures because the low cohesion with respect to the undeformed host rock causes them to be more easily reactivated (Anderson, 1951; Bott, 1959). When deformation propagates, the growth of fault zones is produced by stress concentrations at the boundaries of previous fault surfaces (Scholz, 2002), and the larger the fault, the higher the magnitude of the related earthquakes (Wells & Coppersmith, 1994). The activity of a fault requires the shear stress on its surface to exceed the values of cohesion and friction (Hajiabdolmajid et al., 2002). On a fault surface, the cohesion is low and needs lower shear stresses than on the new developing fault segments at the edge of the previous fault (Hajiabdolmajid et al., 2002). Thus, the propagation of a fault in unfractured resistant rocks can imply a high accumulation of elastic energy that may generate earthquakes of magnitudes higher than those triggered by a reactivation of previous fractures.

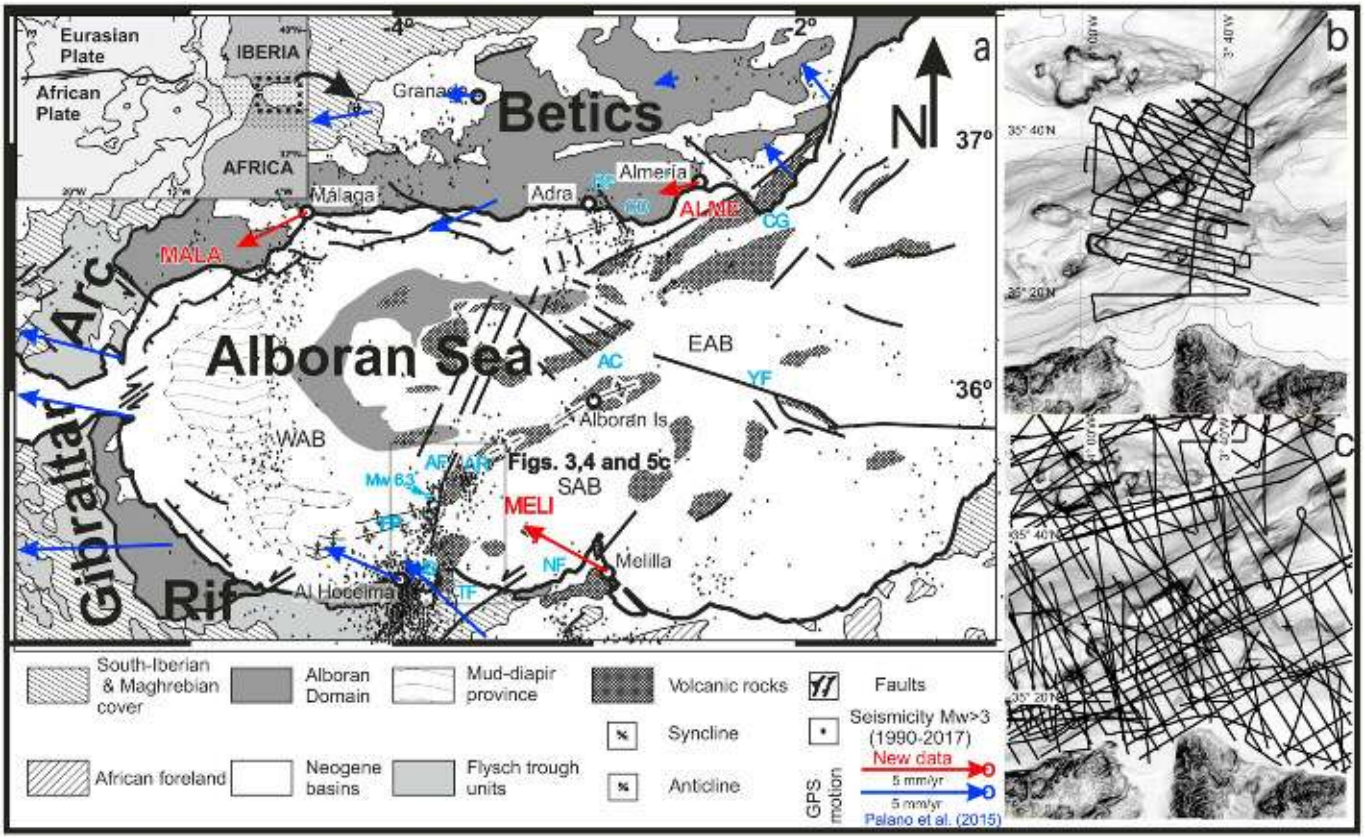

Figure 1. Geological setting including regional faults and seismicity. (a) Plate boundaries in the Azores-Gibraltar area (modified from Galindo-Zaldívar et al., 2003) and geological sketch of the main structural features and basins of the Alboran Sea (modified from Comas et al., 1999). Displacement of GPS stations around the Alboran Sea with respect to stable Eurasia are indicated (red arrows). The dotted area within the inset indicates the deformation area. (b) Tracklines of multibeam, very high resolution seismics (TOPAS) and gravity surveyed simultaneously during the INCRISIS cruise. (c) Tracklines of single-channel and multichannel seismics (airguns) from the ICM database (http://gma.icm.csic.es/sites/default/files/geowebs/OLsurveys/index.htm). Legend: AF, Al Idrisi Fault; AR, Alboran Ridge; AC, Alboran Channel; BF, Balanegra Fault; CD, Campo de Dalías; CG, Cabo de Gata; EAB, East Alboran Basin; FP, Francesc Pagès seamount; NB, Nekor Basin; NF, Nekor Fault; SAB, South Alboran Basin; TF, Trougout Fault; WAB, West Alboran Basin; YF, Yusuf Fault.

The Eurasian-African plate boundary in the Alboran Sea (westernmost Mediterranean) offers a unique research opportunity in a natural example that can provide insights as to the propagation of fault zones (Cowie & Scholz, 1992; Figure 1). The Alboran Basin is a Neogene-Quaternary extensional basin located within the Betic (Spain)-Rif (Morocco) alpine cordilleras, connected by the Gibraltar Arc (Andrieux et al., 1971). The major Trans-Alboran Shear zone (Frasca et al., 2015; Larouzière et al., 1988) accommodated the westward displacement of the Betic-Rif orogen during the development of the Gibraltar Arc. The Alboran Basin is floored by a thin continental crust made up of the alpine Internal Zone metamorphic complexes, with a Variscan basement located in the southeastern area (Ammar et al., 2007) resting above an anomalous mantle (Comas et al., 1992; Hatzfeld, 1976). The sedimentary infill consists of unconformable Miocene to Quaternary deposits (Comas et al., 1992; Juan et al., 2016). This sedimentary record is mostly deformed by two conjugated sets of dextral WNW-ESE and sinistral NE-SW faults and folded by ENE-WSW oriented folds (Estrada et al., 2018; Martínez-García et al., 2017), the Alboran Ridge and Francesc Pagès seamount, pertaining to the main antiforms (Bourgois et al., 1992). The growth of faults and folds takes place in the framework of recent NNW-SSE shortening and regional Eurasian-African plate convergence (de Mets et al., 2015). The Eurasian-African plate boundary shows N-S to NW-SE convergence at present (Fadil et al., 2006; Koulali et al., 2011; Palano et al., 2015), at a rate of 4.93 mm/yr (Argus et al., 2010). Regional present-day ENE-WSW extensional stress is coeval with orthogonal compression, and main stress axes are inclined (de Vicente et al., 2008; Stich et al., 2010).

The Betic-Rif Cordillera and Alboran Sea are affected by a 300-km broad and heterogeneous seismicity band related to the Eurasian-African plate boundary (Buforn et al., 1988). Seismicity generally occurs at shallow

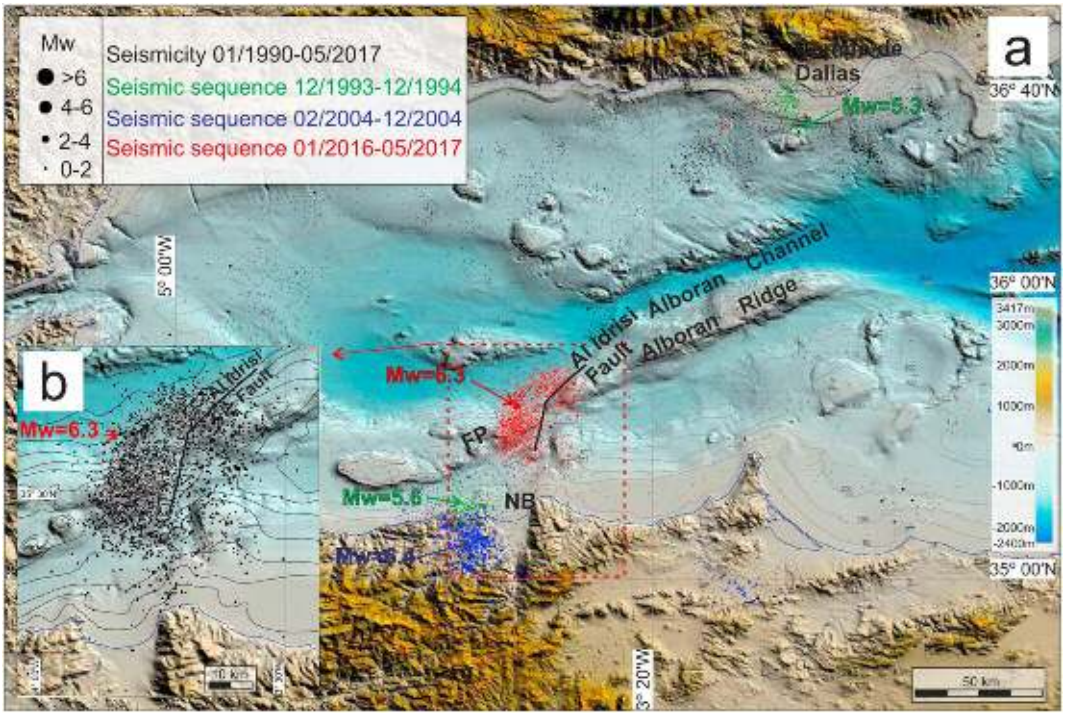

Figure 2. Seismicity distribution during the 2016–2017 seismic sequence and other recent seismicity (including 1993–1994 and 2004 series; (2004 seismic sequence from Van der Woerd et al., 2014; other seismicity from www.ign.es database). (a) Epicenters considering a standard velocity model. (b) Relocated epicenters for the highest-magnitude earthquakes of the 2016–2017 seismic sequence according to El Moudnib et al. (2015). Legend: FP, Francesc Pagès seamount; NB, Nekor Basin.

crustal levels (Buforn et al., 1995). Intermediate seismicity (40 to 120-km deep) is mainly located along a N-S elongated band in the western Alboran Basin that becomes NE-SW northward (Buforn et al., 2017; López-Casado et al., 2001; Medina & Cherkaoui, 2017; Morales et al., 1999). Deep seismicity (600 to 640-km deep) is scarce but also occurs beneath the central Betic Cordilleras (Buforn et al., 1991, 2011). The area has heterogeneous local stresses probably due to fault interaction (Stich et al., 2010).

Several geodynamic models have been proposed for the region, including delamination (e.g., Lis Mancilla et al., 2013; Seber et al., 1996) or subduction with or without rollback (e.g., González-Castillo et al., 2015; Gutscher et al., 2012; Pedrera et al., 2011; Ruiz-Constán et al., 2011; Spakman et al., 2018), yet discussion remains alive. Moreover, in the central and eastern Alboran Sea, the recent fault system mainly composed by two conjugate WNW-ESE dextral and NNE-SSW sinistral fault sets evidences the activity of continental indentation tectonics (Estrada et al., 2018). Within this structural framework, a present-day zone of deformation with high seismic activity crossing the Alboran Sea—from Al Hoceima in the Rif to Adra and Cabo de Gata in the Betics—(Figure 1) oblique to the previous Trans-Alboran Shear zone (Larouzière et al., 1988) has been proposed to be a main plate boundary (Fadil et al., 2006; Grevemeyer et al., 2015). However, relationships with the main tectonic structures observed in the seafloor have not yet been analyzed in detail. The few available studies (Martínez-García et al., 2013, 2017, and references herein; Estrada et al., 2018) suggest that the NNE-SSW sinistral Al Idrisi Fault is the main structure with recent and present-day activity in the southern Alboran Sea (Figure 1). This fault is connected onshore with the Trougout Fault in the Al Hoceima region (Morocco margin), which bounds the Nekor Basin (d'Acremont et al., 2014; Lafosse et al., 2017), and its propagation toward the Rif is discussed by Galindo-Zaldívar et al. (2009, 2015) and Poujol et al. (2014). The Al Hoceima region is deformed mainly by faults that determine a succession of horsts and grabens, probably developed above crustal detachments (Galindo-Zaldívar et al., 2009, 2015). In the northern Alboran Sea, the fault zone extends onshore toward the Campo de Dalías area, connecting with the Balanegra Fault in the boundary of the Betic Cordillera and Alboran Sea (Marín-Lechado et al., 2010).

The 25 January 2016 marked the onset of a seismic sequence in the central southern Alboran Sea (www.ign.es), with a main shock of M_w = 6.3 (Figures 1 and 2) and whose activity continues up to 2017. The area

affected extends from the Francesc Pagès seamount and westernmost Alboran Ridge to the Nekor Basin. The main earthquake was felt in several coastal cities of northern Morocco and southern Spain, causing economic losses in both countries (http://www.ign.es/resources/noticias/Terremoto_Alboran.pdf). The earthquakes of this seismic sequence have been analyzed in detail by the IGN (www.ign.es), Buforn et al. (2017), Medina and Cherkaoui (2017), and Kariche et al. (2018). They consider different velocity models for epicenter locations, suggesting that activity occurred in the area nearby Al Idrisi Fault, yet they do not compare their results with the more accurate position of this fault obtained by marine geophysical research (Estrada et al., 2018; Lafosse et al., 2017; Martínez-García et al., 2013, 2017). The comparison of seismological and marine geophysical researches clearly shows that the epicenters of the earliest stage of the sequence are located to the west of the Al Idrisi Fault.

This paper offers a multidisciplinary analysis of the recent and active near-surface tectonic deformations related to the 2016–2017 seismic sequence within the greater context of the 1993–1994 and 2004 sequences in the central Alboran Sea. Our contribution provides insights into the propagation of recent fault zones and how they are linked to seafloor deformations in addition to their relationships with the former Al Idrisi Fault.

2. Methodology and Data

The combination of different geodetic and geophysical data made it possible to map the area affected by the 2016–2017 seismic sequence, from the deep structure to near-surface morphology and the overall geodynamic setting.

2.1. Regional GPS Data

Permanent GPS stations surrounding the central Alboran Sea served as the reference for present-day deformation in the region. MALA and ALME stations (respectively by Malaga and Almeria) along the Betic Cordillera coast, and MELI (by Melilla) on the African coast, time series were obtained from the EUREF permanent Network. Data were considered up to June 2017, and these stations were in operation: ALME since 2001, MALA since 2005, and MELI since 2012. Global Navigation Satellite System (GNSS) data were processed by means of Bernese Software to determine the displacement vectors.

2.2. Seismicity Data

The seismicity database of the Spanish National Geographic Institute (IGN) (www.ign.es) registered the 2016–2017 seismic sequence and the two previous main seismic series, in 1993–1994 and 2004. The 2004 seismic sequence was carefully relocated by Van der Woerd et al. (2014). As the precise location of seismicity is sensitive to velocity models and to the distance of the seismic stations (Michelini & Lomax, 2004), literature (Buforn et al., 2017; Kariche et al., 2018; Medina & Cherkaoui, 2017) shows a noncoincident location for the 2016–2017 seismic sequence' epicenters. The 1993–1994 and 2016–2017 seismic sequences' epicenter and hypocenter locations were calculated through a standard procedure considering the first arrivals of *P* and *S* waves and a standard velocity model (Carreño-Herrero & Valero-Zornoza, 2011). A careful relocation of the main events was provided by Buforn et al. (2017) and the IGN (IGN, 2016; www.ign.es) in light of the standard and recent velocity model (El Moudnib et al., 2015). Earthquake focal mechanisms were also obtained from the IGN database (www.ign.es), established from first arrival *P* wave polarity. The present-day stress tensor was determined from seismicity using the method by Michael (1984), improved by Vavryčuk (2014).

2.3. Marine Geophysics

The area affected by the 2016–2017 seismic series was surveyed during the INCRISIS cruise on board the R/V Hesperides in May 2016. A dense grid of 31 survey lines, with a total length of about 900 km, was designed taking into account the regional water depths and the general orientation of the morphological and structural features (Figure 1b). Data positioning was determined via a Global Positioning System (GPS). The studied area was covered by a multibeam SIMRAD EM120 echosounder (frequency 12 kHz) that enabled us to record high-resolution bathymetry. Vertical resolution was approximately 0.025% of water depth. CARIS Hips software was used for multibeam data processing. This bathymetry was integrated with previous data sets in the area (http://gma.icm.csic.es/sites/default/files/geowebs/OLsurveys/index.htm) and gridded at 25 m.

Simultaneously with multibeam bathymetry, very high resolution seismic profiles were acquired with the SIMRAD TOPAS PS18 system (frequencies of 18 kHz to 1 to 6 kHz). In addition to this information, multichannel and single-channel seismic records from the Instituto de Ciencias del Mar-CSIC database (http://gma.icm.csic.es/sites/default/files/geowebs/OLsurveys/index.htm) were considered (Figure 1c). All seismic profiles were integrated into a Kingdom Suite project (IHS Kingdom) for their correlation and interpretation. Likewise, gravity data were obtained during the INCRISIS cruise using a Lockheed Martin BMG3 marine gravimeter with a precision of 0.7 mGal. Gravity Free air and Complete Bouguer anomalies were determined considering a standard density of 2.67 g/cm^3. To extend the gravity anomalies to the shoreline, we used the global free air data set from Sandwell et al. (2014). Directional filters (horizontal gravity gradient) were applied in order to analyze the main tectonic structures.

3. Results

The area affected by the 2016–2017 seismic sequence is located in the southern sector of the Alboran Sea central part (from 125 to 1,450-m water depth), from the Nekor Basin to the vicinity of Alboran Ridge and Francesc Pagès seamount (Figures 1 and 2). The northern steep side of the Alboran Ridge gives way abruptly to the Alboran Channel, whereas that of the Francesc Pagès seamount evolves to flat-lying seafloor of the deep basin through a terraced-shaped sector that parallels the seamount.

3.1. Present-Day Alboran Sea Shortening From GPS Data and Plate Deformation

Deformation within the Alboran Sea is driven in part by the NW-SE regional convergence of the Eurasian and African plates (de Mets et al., 2015). The west to west-southwestward motion of the Betic-Rif Alboran block (Koulali et al., 2011; Palano et al., 2015) may also be the result of ongoing slab rollback toward the west (González-Castillo et al., 2015; Gutscher et al., 2012; Pedrera et al., 2011; Ruiz-Constán et al., 2011; Spakman et al., 2018), which would explain the E-W to ENE-WSW extensional focal mechanisms observed in the West Alboran Sea (Stich et al., 2010). At present, the GEODVEL plate model (Argus et al., 2010) indicates a N141°E trend of convergence at a rate of 4.93 mm/yr in this region, supported by regional GPS data (Fadil et al., 2006). This regional deformation produces a NNW-SSE shortening, which, in the central part of the Alboran Sea, may be constrained by the MALA and ALME stations in Spain and by MELI station in Morocco (Figure 1). The higher rates of MALA station with respect to ALME evidence ENE-WSW extension in the Betic Cordillera (Galindo-Zaldivar, Gil, et al., 2015). The southern displacement of ALME and MALA stations relative to the European Plate contrasts with the northern displacement of MELI, supporting present-day shortening in the central Alboran Sea. The most intensely seismic area in 2016–2017 is located in between MALA and MELI stations, with a relative NNW-SSE (N173°E) shortening of 3.3 mm/yr.

3.2. Recentmost Seismic Sequence

A seismic zone of intense activity affects the central Alboran Sea, from the Campo de Dalias region in the north to the Al Hoceima region in the south (Figures 1 and 2), it being most intense at the southern end (Grevemeyer et al., 2015). The most recent seismic sequences were in 1993–1994, 2004, and 2016–2017 (Figure 2). The 1993–1994 seismic sequence affected the coastal region nearby Al Hoceima, with a main earthquake of M_w = 5.6 (26 May 1994), after an earlier earthquake in the Campo de Dalías area, of M_w = 5.3 (23 December 1993). In 2004, another seismic sequence with a devastating earthquake event of M_w = 6.4 (24 February) occurred onshore in the Al Hoceima region causing nearly 600 deaths and with aftershocks reaching the Alboran Sea (Van der Woerd et al., 2014). Earthquake focal mechanisms were very similar in all cases, pointing mainly to sinistral strike slip along the NNE-SSW oriented deformation zone (El Alami et al., 1998; Stich et al., 2006, 2010), although also possible is the activity of WNW-ESE dextral faults in the 2004 sequence that affect Al Hoceima onshore areas (Akoglu et al., 2006; Van der Woerd et al., 2014).

The 2016–2017 seismic sequence (Figures 2 and 3) was initiated by a moderate earthquake (21 January 2016, M_w = 5.1) followed closely by a stronger event (25 January, M_w = 6.3) and by a long seismic series of decreasing activity during 2016–2017 (Buforn et al., 2017; Kariche et al., 2018; Medina & Cherkaoui, 2017). The relatively long distances from hypocenters to seismic stations, generally greater than 50 km and in some cases reaching more than 80 km, decrease the quality of earthquake locations. Buforn et al. (2017) recognize average horizontal errors of 5 km and vertical errors of 10 km, comprised between 2 to 10 km horizontally and 3 to 17 km vertically. The location of 2016–2017 seismic activity established by the IGN standard terrain velocity

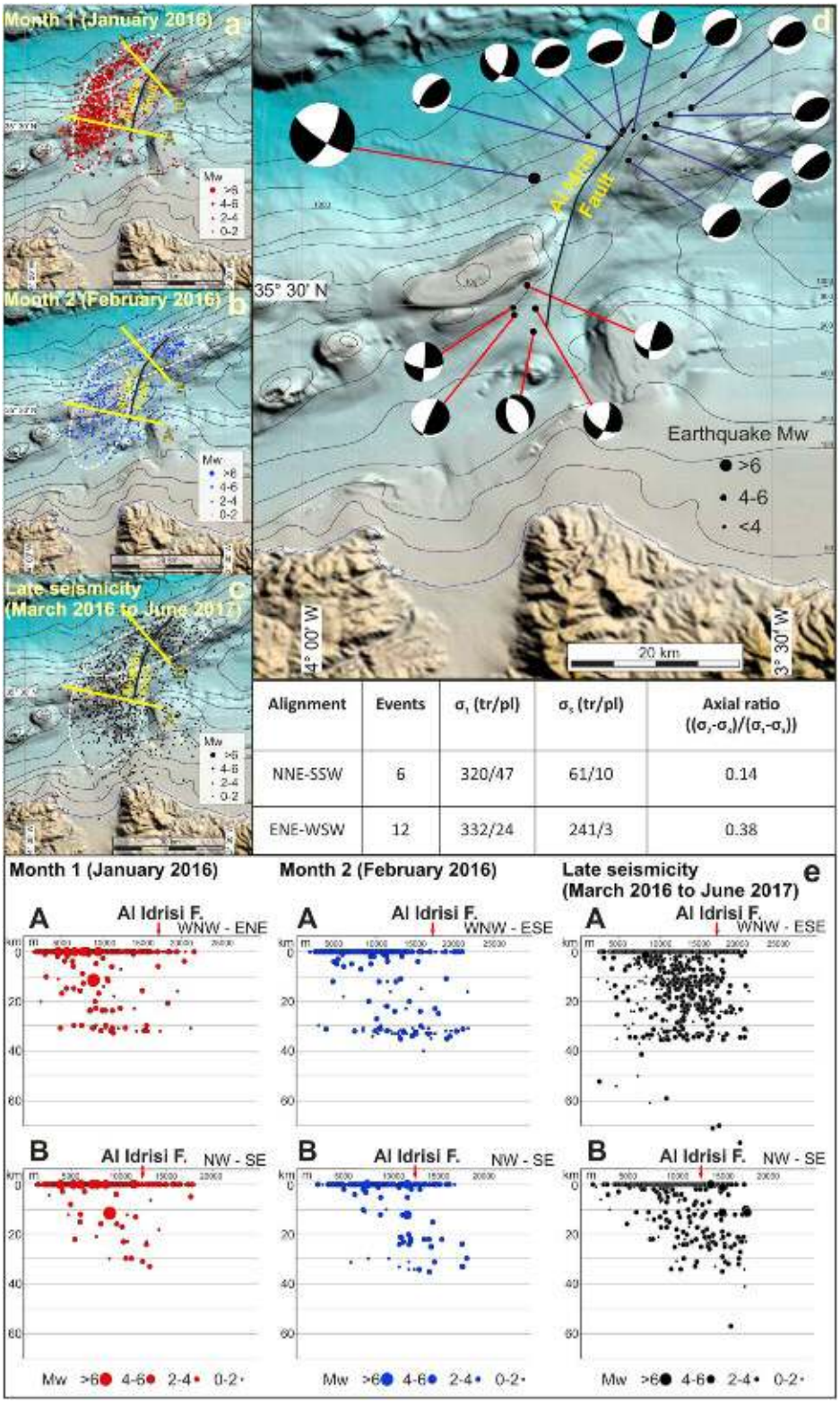

Figure 3. Seismicity during the 2016–2017 seismic sequence. (a) Epicenters month 1 (January 2016). (b) Epicenters month 2 (February 2016). (c) Late epicenters (March 2016 to June 2017). (d) Earthquake focal mechanisms from 2016 to 2017 seismic crisis (data from IGN, www.ign.es). NNE-SSW alignment in red, ENE-WSW alignment in blue. The main earthquake, located at the edge of the two alignments, is shared by the two groups. Present-day stress is determined in the two main sectors of 2016–2017 Alboran Sea seismic crisis area (by the methods of Michael, 1984; improved by Vavryčuk, 2014). (e) Cross sections of seismic activity orthogonal to the main alignments.

model (Carreño-Herrero & Valero-Zornoza, 2011; Figures 2a and 3) or El Moudnib et al. (2015) velocity model (Figure 2b) shows a deformation band with two alignments, the main one, oriented NNE-SSW, changing sharply to an ENE-WSW trend. Considering the IGN standard terrain velocity model (Carreño-Herrero & Valero-Zornoza, 2011; Figures 2a and 3), the NNE-SSW alignment is about 40 km in length and 10–20-km wide and includes shallow earthquakes (<35-km depth) that affect the crust and upper mantle. It is parallel and significantly displaced westward (up to 10 km) with respect to the Al Idrisi Fault (Figure 2). The ENE-WSW alignment, about 20-km long and 10–15-km wide, is located along the northern side of the westernmost Alboran Ridge and the Francesc Pagès seamount and is also characterized by a shallow seismicity (<35 km). During month 1 (January 2016), the seismicity clearly defines the two alignments with widths of less than 10–20 km, the main southern one being displaced 5 to 10 km westward with respect to the trace of the main Al Idrisi Fault (Figures 2 and 3a). During month 2 (February 2016), seismic activity decreases and both alignments become wider (10–20 km; Figure 3b). Then, from month 3 (March 2016) to present, seismicity gradually decreased and affected a broader area, more than 15–25-km wide (Figure 3c), in between the one clearly defined in month 1, and bounded eastward by the main trace of Al Idrisi Fault. Buforn et al. (2017) relocate the earthquakes considering El Moudnib et al. (2015) velocity model and also obtain the same pattern formed by two alignments, the NNE-SSW with a westward offset with respect to the Al Idrisi Fault sea bottom location.

The earthquake focal mechanisms of the two seismicity alignments show different behaviors (Figure 3d). The main NNE-SSW alignment is characterized by sinistral earthquake focal mechanisms related to NNE-SSW subvertical faults, roughly parallel to the elongation of the alignment. There is also heterogeneity of earthquake focal mechanisms with inclined *P* and *T* axes and normal faults, supporting ENE-WSW extension toward the southern deformation zone. In contrast, the ENE-WSW alignment is characterized by highly homogeneous reverse earthquake focal mechanisms associated with ENE-WSW faults. Present-day stress (Figure 3) supports low NNW (N320°E to N332°E) inclined compression and orthogonal horizontal extension in both segments linked to prolate stress ellipsoids. Inclination is higher (47°) in the main alignment and its axial ratio is closer to triaxial stress.

3.3. Deep Structure From Gravity Data

Bouguer complete gravity anomalies decrease in the Alboran Sea, from 110 to 30 mGal, in a smooth transition from the east to the west up to 4.5°W (Casas & Carbó, 1990). As the amplitude decreases, it narrows to the west, so that the greatest values are located in the central part.

The Bouguer complete anomaly map of the 2016–2017 seismic sequence area and its surroundings shows values between 100 and 10 mGal. Despite some isolated highs, the values decrease progressively from north in the central Alboran to south in the Moroccan margin. Bouguer anomaly highs in the central Alboran (northern part of Figure 4a) support the presence of a local thinning of the continental crust (Galindo-Zaldivar et al., 1998). The shaded relief of the complete Bouguer anomaly map with illumination from the east (Figure 4b) is sensitive to N-S trends and tracks the extension of alignments coming out of Nekor Basin, at least as far as the Alboran Ridge. One alignment (labeled "B" in Figure 4b) nearly parallels the Al Idrisi Fault, though displaced westward. The plots of the 2016–2017 epicenters of earthquakes having magnitude over 3.9, once relocated, show that the southern sector lies over the alignment located in the middle.

3.4. Recent and Active Near-Surface Tectonic and Sedimentary Deformations

The morpho-bathymetric and seismic analysis of the near-surface sediments affected by the 2016–2017 seismic sequence provides evidence of recent and active faults, as well as folds and mass transport deposits (MTDs; Figures 5–9). MTDs are located on the northern side of the Francesc Pagès seamount and Alboran Ridge, along the ENE-WSW active seismicity alignment and the main earthquake (Figures 5 and 6). Based on the thickness of remobilized sediment, small-scale MTDs (a few ms thick) and large-scale MTDs (tens of ms thick) were identified.

The small-scale MTDs occur mostly on the relatively steep slopes (~ < 5°) of the northern side of both seamounts, from >250 to 1,000-m water depth. They appear as vertically stacked subtabular units (a few tens of milliseconds) of unconsolidated deposits and lenticular and irregular bodies of semitransparent, contorted, and discontinuous stratified facies, separated by relatively high reflectivity surfaces with local hyperbolic

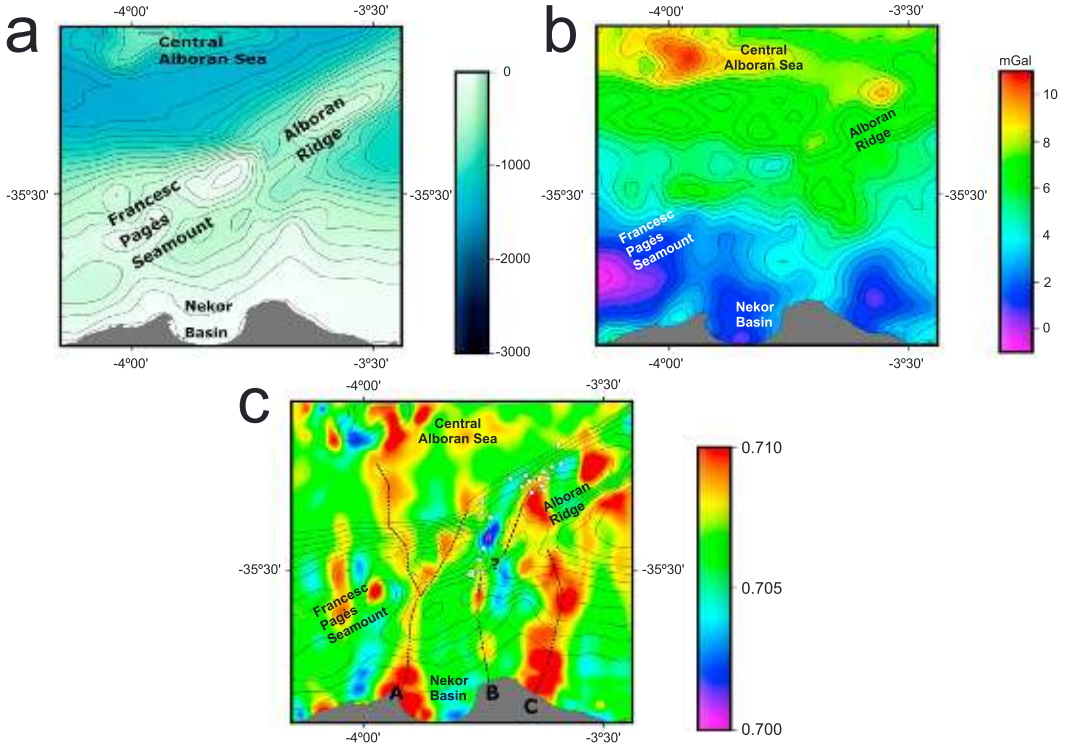

Figure 4. Gravity anomaly maps and main tectonic features. (a) Bathymetry map, contour lines every 100 m. (b) Complete Bouguer gravity anomaly map at 2-km resolution. Contour lines every 5 mGal. (c) A shaded relief map (illuminated from the east) of the complete Bouguer gravity anomaly. Black dashed lines denote offshore N-S alignments (labeled as A, B, and C); white dots mark earthquakes with magnitude >3.9; thin contour lines represent bathymetry.

echoes. The strata pattern suggests the recurrent nature of gravity drive transport. These facies conform an irregular seafloor surface with gentle undulations (metric in scale). The large-scale MTDs mainly occur seaward with respect to the previous ones and extend down to the deep basin (as much as 1,450-m water depth). They are related to slide scars, most of them removing the small-scale MTDs. The slide scars display an amphitheater shape (up to 1-km wide, 40-m relief) recognizable at seafloor, where they extend along a fringe at the foot of the Francesc Pagès seamount. Most of these MTDs are detached from the slide scars and are acoustically defined by lenticular bodies (up to 55-ms thick) internally characterized by semitransparent and discontinuous stratified facies and having a distinctive irregular seafloor surface recognized bathymetrically. Their acoustic character indicates disintegration of the removed mass, just after the initiation of mass flow-type movement. Seismic records also provide evidence of buried large-scale MTDs that interrupt and erode the surrounding basinal undeformed stratified facies, suggesting the episodic nature of such slope sedimentary instabilities, at least in recent geological times. Their stratigraphic position points to a simultaneous occurrence of some MTDs (Figure 6).

With respect to the folds, the Alboran Ridge and Francesc Pagès seamount constitute the main antiformal structures deforming the region (Figures 5 and 7). The ENE-WSW folds affect Miocene age deposits (Martínez-García et al., 2013). The fold geometry is irregular, with variable wavelengths (kilometer in scale) and vergences (NNW or SSE). In addition, smaller-scale folds (hundreds of meters in scale) are identified in relation to the Al Idrisi Fault (Figure 8), with axes oriented parallel to it.

The main fracture of morphological and seismic expression, deforming the most recent sediments, is the sinistral Al Idrisi Fault zone (Martínez-García et al., 2011, 2013, 2017; Figures 5 and 8). This fault has a 50-km-long northern segment with N35°E trend. It develops a recent fault scarp of about 20 to 30 ms (15 to 23 m) at the northwestern edge of the Alboran Ridge that constitutes the upthrown block (Figures 5 and 8). In the hanging wall, small-scale MTDs are recognized. The near-surface sediments in this sector are affected by folds. Al Idrisi Fault changes its direction suddenly to N15°E in the area between the Francesc Pagès

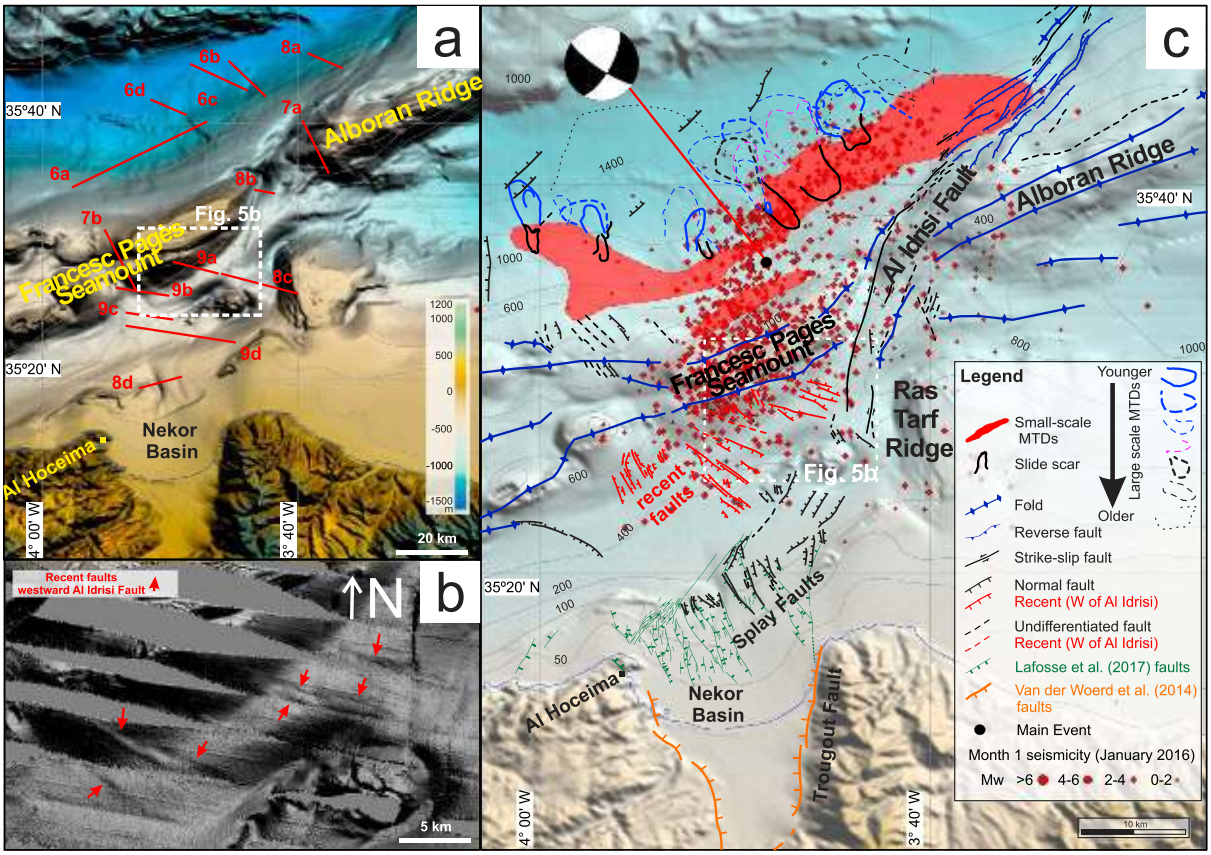

Figure 5. Recent sea bottom deformation affecting the 2016–2017 Alboran Sea seismic active area: MTDs, faults, and folds. (a) INCRISIS bathymetry integrated with previous datasets in the area (http://gma.icm.csic.es/sites/default/files/geowebs/OLsurveys/index.htm). Data are gridded at a resolution of 25 m. (b) Detailed view of recent fault scarps mapped during the INCRISIS multibeam bathymetry. The gray plain areas were not covered by the multibeam echosounder. (c) Geomorphological and tectonic map. The INCRISIS TOPAS seismic profiles were also integrated with the multichannel and single-channel seismic records from the Instituto de Ciencias del Mar-CSIC database (http://gma.icm.csic.es/sites/default/files/geowebs/OLsurveys/index.htm). The 2016 seismicity is from www.ign.es database.

seamount and the westernmost end of the Alboran Ridge. Here it is characterized by a sharp elongated depression covered by undeformed recent sediments. The main N15°E southern segment is about 20-km long and extends discontinuously southward, toward the Nekor Basin in relay with the Trougout Fault, forming splay faults (Lafosse et al., 2017). The southern end of Al Idrisi Fault trace is located at a deformation zone with smaller faults reaching the sea bottom (Figure 5). Previous research of earthquake focal mechanisms (Grevemeyer et al., 2015; Martínez-García et al., 2011, 2013, 2017) suggests a sinistral slip on the Al Idrissi Fault NNE-SSW vertical fault plane, further confirmed by the short displacement, roughly 5 km, of the antiformal axis of Alboran Ridge with respect to the Francesc Pagès seamount (Martínez-García et al., 2011, 2013, 2017).

Our new geomorphological and tectonic map evidences, for the first time, a recent fault zone to the north of the Nekor Basin affected by the 2016–2017 seismic sequence (Figures 5 and 9). It is located approximately 5 to 10 km westward of the Al Idrisi Fault, south of Francesc Pagès seamount. Its bathymetric expression (a few meters of relief) correlates with the epicentral area. The faults have NW-SE orientation, with high northeastward or southwestward dips. The very high resolution seismic images of this recent fault zone suggest that they are grouped in conjugate faults with a normal component affecting the most recent sediments, some of them reaching up to the seafloor (Figure 9).

4. Discussion

This multidisciplinary focus on the 2016–2017 seismic sequence in the Alboran Sea—in the wake of previous sequences in 1993–1994 and 2004, and the former Al Idrisi Fault—sheds light on the seafloor deformation

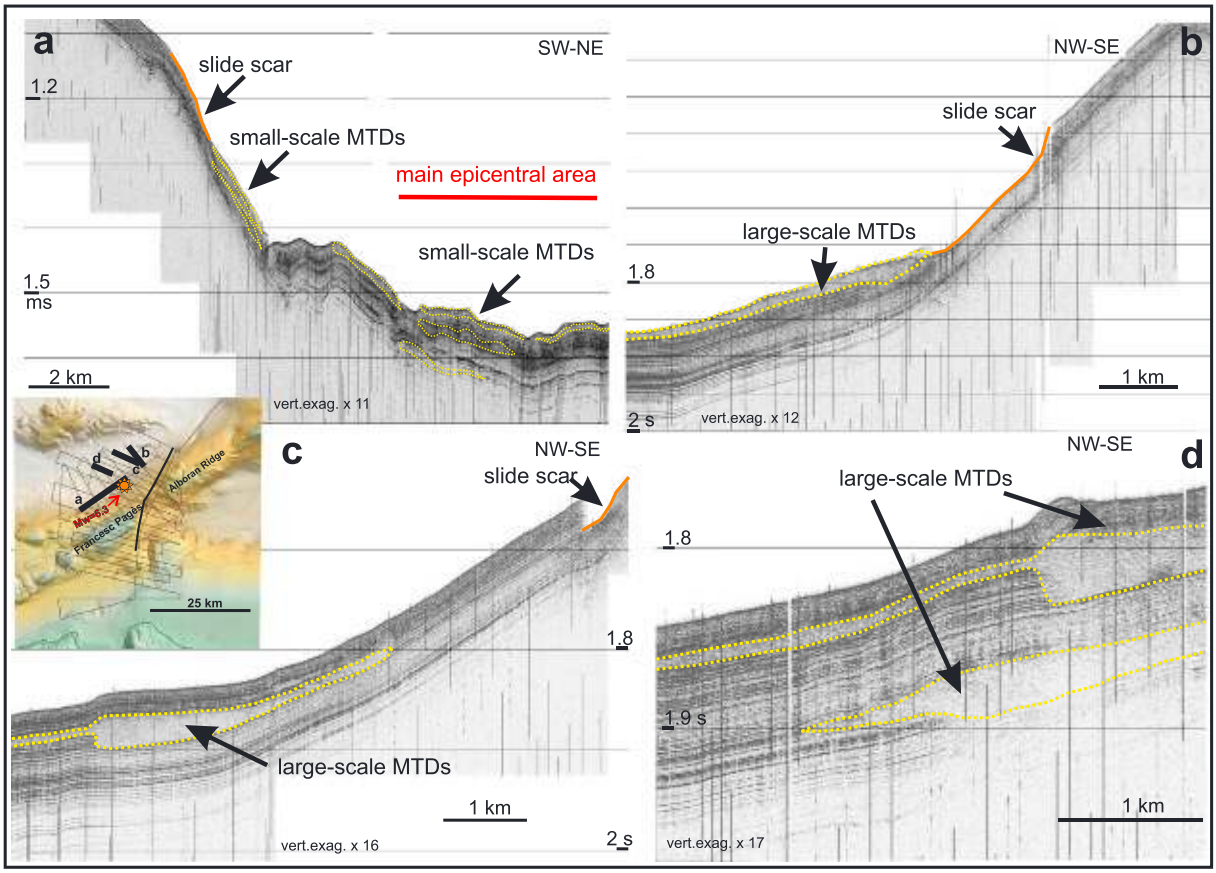

Figure 6. Segments of TOPAS seismic records displaying the small- and large-scale MTDs mapped in the ENE-WSW seismicity alignment. Thin vertical discontinuous lines, noise.

and relevant implications in terms of geological hazard. The results help to constrain the processes that occur during migration and propagation of active tectonic brittle deformations.

4.1. Constraining Active Tectonics: Seismicity and Seafloor Deformations

Epicenters related to wrench faults are expected to be located along the fault zone trace. Vertical nodal planes of earthquake focal mechanisms from the main 2016 earthquake and most of the events in the southern Alboran Sea undoubtedly evidence the vertical dip of the seismic active faults (Figure 3), in

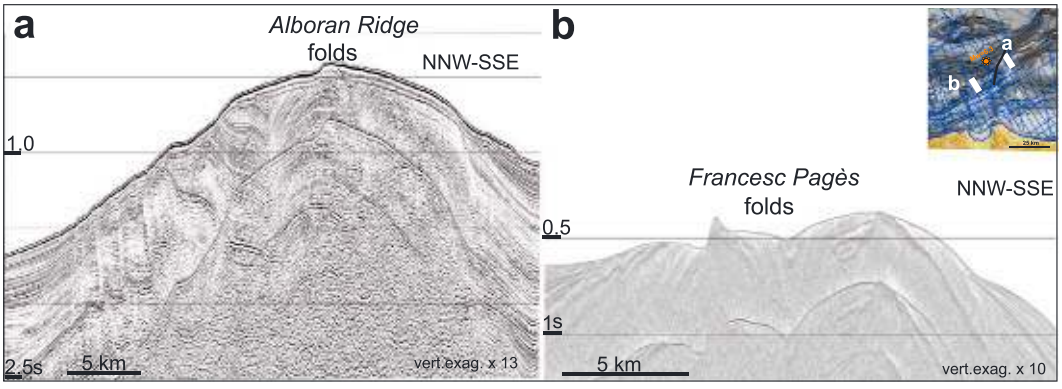

Figure 7. Segments of multichannel seismic records displaying the (a) Alboran Ridge and (b) Francesc Pagès seamount folds.

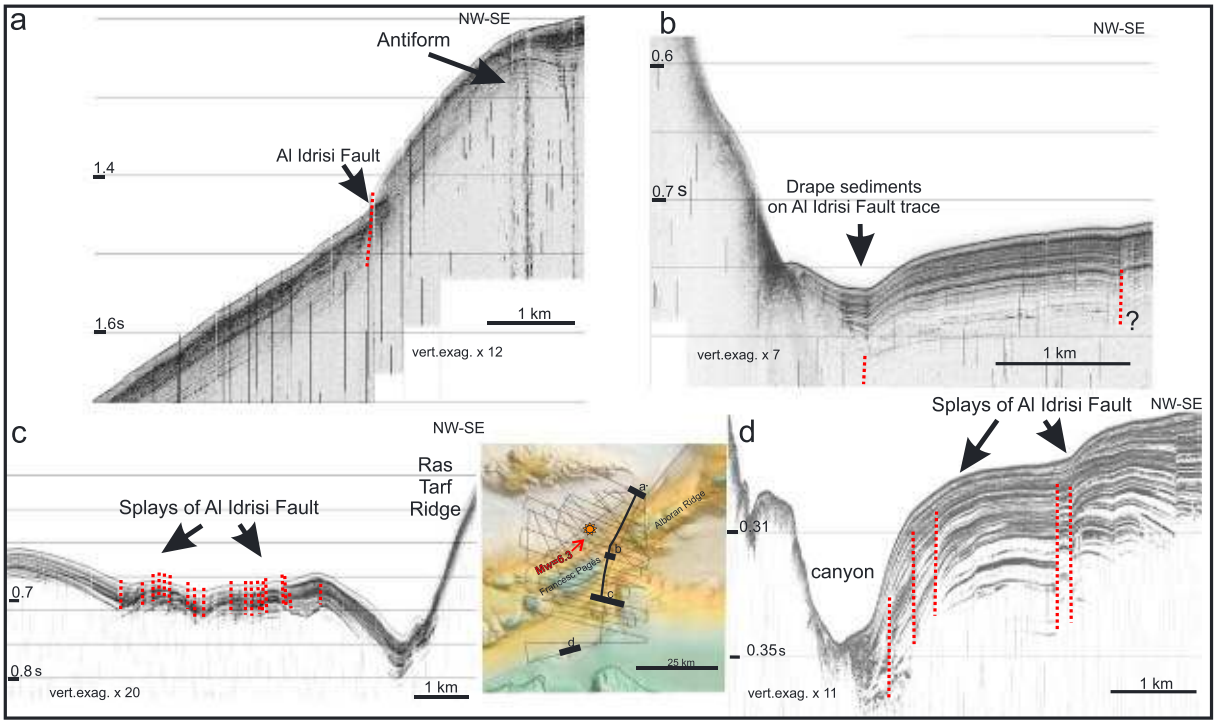

Figure 8. Segments of TOPAS seismic records displaying the Al Idrisi Fault deformation along its trace. The fault generally affects recent sediments, although undeformed sediments cover the central part of the fault trace. Thin vertical discontinuous lines, noise.

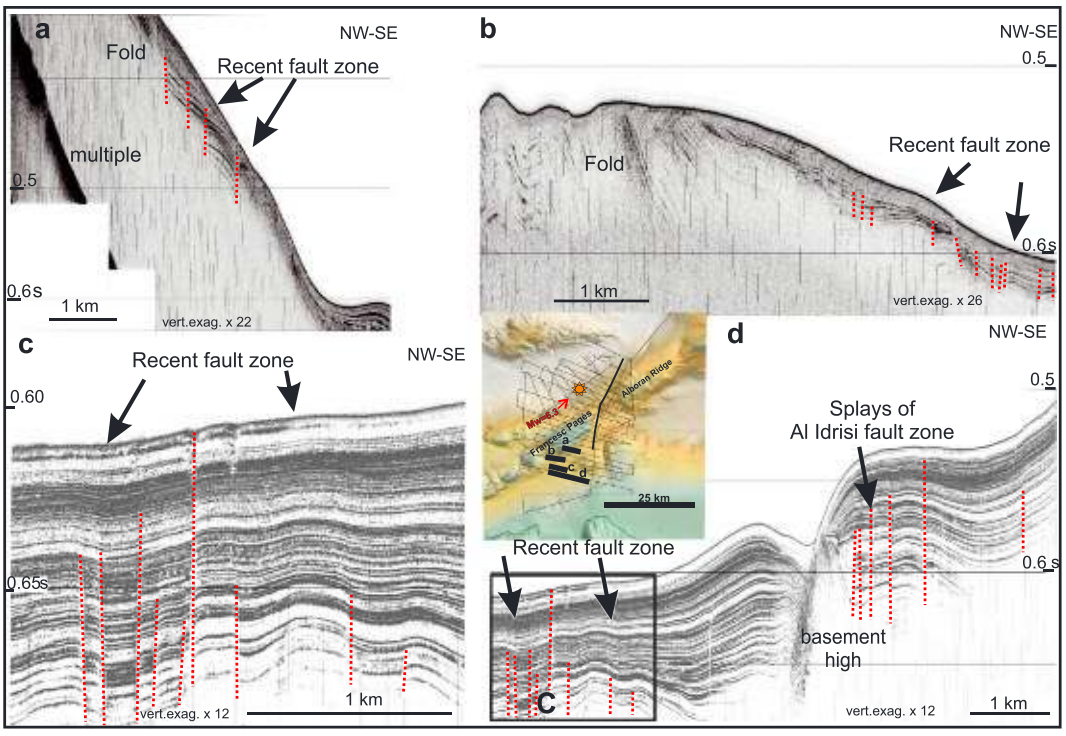

Figure 9. Segments of TOPAS seismic records displaying the recent fault zone identified in this study. This zone is located 5 to 10 km westward of the Al Idrisi Fault (d). Thin vertical discontinuous lines, noise.

agreement with the seismological results of Buforn et al. (2017). Anyway, aftershock sequences can affect a wide zone (e.g., >10-km wide with respect to the main fault during the Landers 1992 seismic sequence; Hauksson et al., 1993) favored by the structural complexity and preexisting structures. Despite that Buforn et al. (2017) establish horizontal and vertical errors for the 2016–2017 seismic sequence location, and Buforn et al. (2017) and Medina and Cherkaoui (2017) relate the seismicity with the Al Idrisi Fault, the careful analyses of epicenter locations for most of the NNE-SSW seismicity alignment (IGN, www.ign.es; Buforn et al., 2017; Kariche et al., 2018; Medina & Cherkaoui, 2017) point to that they are displaced westward with respect to the seafloor trace of the Al Idrisi Fault determined by marine geophysical data (Estrada et al., 2018; Martínez-García et al., 2013, 2017; Figures 2, 3, and 5). This displacement of the earthquakes is higher when the standard velocity model (Carreño-Herrero & Valero-Zornoza, 2011) is considered (IGN, www.ign.es; Kariche et al., 2018; Medina & Cherkaoui, 2017): roughly 10 km for the first stage earthquakes (Figures 2a and 3a), as opposed to the roughly 5 km (Buforn et al., 2017) with the model by El Moudnib et al. (2015; Figure 2b). Although the mislocation of earthquakes by the poorly constrained velocity models and far seismic stations may produce a westward shift of the seismicity with respect to the Al Idrisi Fault, all the available seismological studies (IGN, www.ign.es; Buforn et al., 2017; Kariche et al., 2018; Medina & Cherkaoui, 2017) support the offset to the west of the seismicity and fault activity with respect to the former Al Idrisi Fault that roughly constitutes the eastern boundary of the fault zone. Our findings based on the marine geophysical data set demonstrate the development of recent faults west of the former Al Idrisi Fault related to the westward propagation of the deformation (Figures 2, 3, and 8–10).

The early earthquakes of the 2016–2017 series are clearly grouped in the two relatively narrow (~10–20-km wide) NNE-SSW and ENE-WSW alignments, starting with the highest magnitude event (M_w = 6.3, 25 January) where they join (Figure 3a). The depth of seismicity is not well constrained because of the variability of crustal velocities and the few and far onshore stations; still, they correspond to crustal levels (<35-km depth), in agreement with Buforn et al. (2017), Medina and Cherkaoui (2017), and Kariche et al. (2018). New seismic faults started to develop at shallow crustal levels (roughly 5 to 10-km depth), as generally occurs in continental crust (Meissner & Strehlau, 1982). If an elliptical fault surface shape is considered (Watterson, 1986), the recent fault should extend in depth northward and southward into the seismogenic crustal layer. When deformation propagates upward, the triggering fault is expected to reach the seafloor in the NNE-SSW epicenters alignment, due to the high dip of fault plane solutions in most of the earthquake focal mechanisms. According to empirical fault scaling relationships (Wells & Coppersmith, 1994), the main seismic event would be related to a surface rupture between 15 and 20 km and might deform the area. In the 2016–2017 seismic series, a recent fault zone (10–20-km wide) reaching up to the seafloor was recognized in the main NNE-SSW seismicity alignment, south of Francesc Pagès seamount. This recent zone comprises NW-SE oriented conjugated normal faults coeval with the recent sedimentation, reaching different near-surface stratigraphic levels, probably rotating and connecting in depth with the major recent NNE-SSW vertical sinistral fault (Figure 10). These shallow faults accommodate the NE-SW extension compatible with the activity of the main wrench fault and are in agreement with crustal thinning in the Nekor Basin confirmed by Bouguer gravity anomalies (Figure 4); they would be in line with the recent normal faults described by Lafosse et al. (2017) that demonstrate that the Nekor Basin is floored by a set of splay faults with normal slip component related to the southern prolongation of Al Idrisi Fault.

During later earthquakes, the 2016–2017 seismic series deformation extended to a broad 10–20-km-wide fault zone in the NNE-SSW alignment, bounded westward by the recent faults and eastward by the Al Idrisi Fault and the Alboran Ridge. Al Idrisi Fault, in contrast, only deforms discontinuously near-surface sediments along the fault trace by recent or active faults and folds, suggesting the recentmost activity of some segments. Although the discontinuous evidences of activity may be the consequence of a seismic character of Al Idrisi Fault, with segments accumulating elastic deformation before the seismic rupture, alternatively, they could indicate that the activity of those segments has been replaced by that of other recent faults offset to the west.

In the ENE-WSW alignment, the morphostructural pattern and deformation behavior are different. The presence of MTDs (Figures 5 and 6) and reverse earthquake focal mechanisms (Figure 3d), and the absence of clear reverse faults affecting the near-surface, would suggest the presence of blind reverse faults at the core of the Alboran Ridge antiform (Figure 10; Martínez-García et al., 2013).

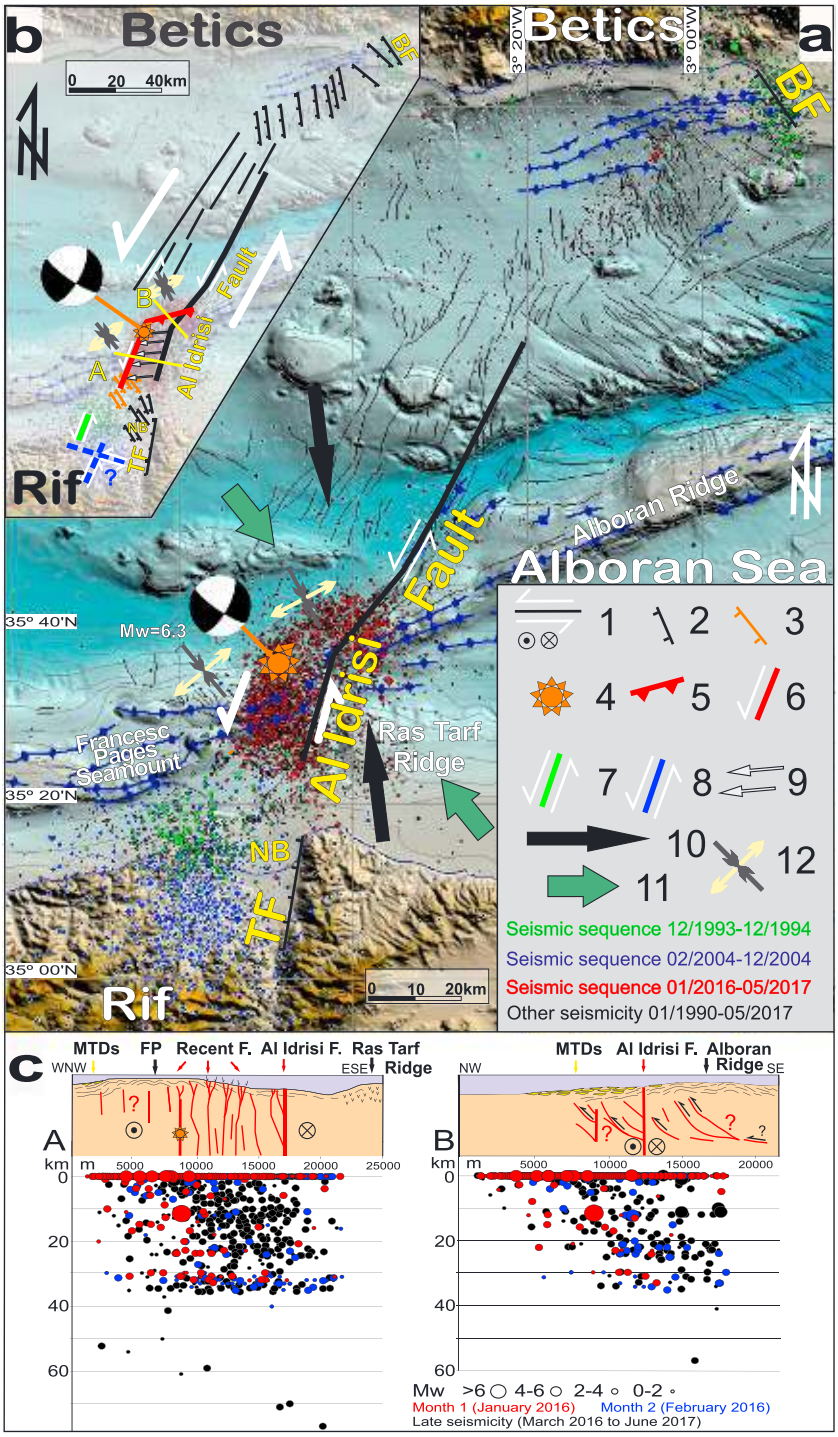

Figure 10. Sketch illustrating the westward propagation of recent tectonic and seismic activity in the main NNE-SSW deformation zone crossing the Alboran Sea. (a) Seismicity, main active structures, stress and shortening. The 2004 seismic sequence from Van der Woerd et al. (2014); other seismicity from www.ign.es database. (b) Sketch of main tectonic structures and westward migration of deformation from main Al Idrisi Fault trace. (c) Interpretative cross sections and seismicity orthogonal to the main earthquake alignments: 1, sinistral fault (map and cross section); 2, normal fault; 3, recent normal fault; 4, epicenter of main event (M_w = 6.3, 25 January 2016); 5, active blind thrust; 6, active NNE-SSW sinistral deep vertical crustal fault segment bounding westwards the NNE-SSW 2016–2017 seismicity alignment; 7, active NNE-SSW vertical sinistral crustal fault segment related to the 1993–1994 seismic crisis; 8, active NNE-SSW vertical sinistral crustal fault segment related to the 2004 seismic crisis; 9, offset to the west of recent deformation and seismicity in respect to Al Idrisi Fault; 10, estimated convergence trend from GPS data; 11, regional plate convergence trend; 12, present-day trends of compression and extension determined from earthquake focal mechanisms. FP, Francesc Pagès seamount. MTD, mass transport deposits.

Earthquakes may be assumed to be the main mechanism triggering the MTDs, deforming the near-surface sediment of the ENE-WSW alignment (Figures 5 and 6; Casas et al., 2011). The initiation of slope failure is due to cyclic loading applied on the sediment and a decreasing shear strength through the development of pore overpressure. Other factors, such as tectonic deformations resulting in seabed, may also contribute to increasing shear stress on the slope or a decreasing sediment strength due to shearing, dilatancy, and possible sediment creep (Locat & Lee, 2002).

4.2. Geodynamic Implications and Seismic Hazard

The former NE-SW sinistral Trans Alboran Shear Zone (Larouzière et al., 1988) constituted a main tectonic structure during the Miocene, later becoming inactive and overprinted by the recent NNE-SSW deformation zone (Stich et al., 2006, 2010) between Campo de Dalías (Balanegra Fault) and the Al Hoceima region (Trougout Fault), including the Al Idrisi Fault (Figure 10). This evolution reveals a progressive offset to the west and rotation of the central Alboran Sea active deformation zone. The recent shear zone has incipient low deformation. Al Idrisi Fault, which constitutes the longest fault in this deformation zone, has short strike-slip, however. It is expressed by low interaction at the edge where the Al Idrisi Fault orientation trace changes and also by the short displacement between the Alboran Ridge and Francesc Pagès seamount antiform axes (Figure 10).

At present, seismological and GPS studies hold the active seismic zone in the central Alboran Sea to be a main weak zone related to the Eurasian-African plate boundary (Buforn et al., 2017; Fadil et al., 2006; Grevemeyer et al., 2015; Medina & Cherkaoui, 2017; Palano et al., 2015). The fact that seismicity occurred near the African coastline in 1994, with maximum magnitude of $M_w = 5.6$ (26 May), and later propagated toward the continent in 2004 with a main event of $M_w = 6.4$ on 24 February (e.g., Akoglu et al., 2006; Van der Woerd et al., 2014, and references therein) would indicate that the 2016–2017 seismicity (main event $M_w = 6.3$) is most likely located within the same regional deformation band (Figures 2 and 10), at its northern edge. Accordingly, the recent fault zone exhibits a segmented behavior with the progressive reactivation of 15–20-km length stretches demonstrated by the recent seismic series (1993–1994, 2004, and 2016–2017; Buforn et al., 2017; Kariche et al., 2018; Medina & Cherkaoui, 2017). In the Rif, seismic faults have rupture in depth but with no clear surface expression (Galindo-Zaldívar et al., 2009; Galindo-Zaldívar, Azzouz, et al., 2015; Van der Woerd et al., 2014). Akoglu et al. (2006) and Van der Woerd et al. (2014) show that seismicity onshore Al Hoceima region has been produced by the activity of NNE-SSW but probably also WNW-ESE conjugated faults in NNW-SSE compression and ENE-WSW orthogonal extensional stresses.

Northward, toward the Betic Cordillera, the deformation zone is connected with the Campo de Dalías and its seismicity during the 1993–1994 series (Marín-Lechado et al., 2005; Figure 10).

The present-day stresses determined from regional seismicity studies (de Vicente et al., 2008; Stich et al., 2010) agree with the data obtained in the context of the 2016–2017 seismic sequence (Figures 3 and 10). The NW-SE compression is prolate to triaxial and inclined toward N319°E in the NNE-SSW seismicity alignment, while N332°E in the ENE-WSW alignment, with related orthogonal extension. Thus, compression is rotated in the two alignments and is compatible with sinistral fault kinematics (Figure 10). Whereas at the Earth's surface, main stresses should be horizontal or vertical due to an absence of shear stress (Anderson, 1951; Bott, 1959), the inclination of main compression toward the NW at crustal depths suggests activity of northwestward thrusting to some extent. Moreover, this setting could be a consequence of the presence of a low-deformed resistant domain attached to the African plate, here corresponding to the external Rif units on the Variscan basement (Estrada et al., 2018; Galindo-Zaldívar, Azzouz, et al., 2015; Pedrera et al., 2011).

There is furthermore some disagreement between the maximum horizontal compression (between N139°E and N152°E) and maximum local shortening (N173°E; Figure 10), estimated by the MALA and MELI GPS stations across the seismic active area. It may be that fault activity is not due to a simple strike-slip fault driven by a far-field stress in the sense of Anderson (1951) but could accommodate crustal block displacement. The NE-SW extension that occurs toward the fault tips, at the northern edge of Campo de Dalías normal faults (Galindo-Zaldívar et al., 2013; Marín-Lechado et al., 2005), is transferred toward the southern edge, where normal faults splay at the Nekor Basin (Figure 10; Galindo-Zaldívar et al., 2009; Lafosse et al., 2017), and crustal thinning is confirmed by gravity results (Figure 4a).

The epicenters of three seismic series are located west of the main faults recognized at surface, both in the Alboran Sea (Al Idrisi Fault) and in the northern Rif (Trougout Fault; Figures 2 and 10; Galindo-Zaldívar et al., 2009; Galindo-Zaldívar, Azzouz, et al., 2015; d'Acremont et al., 2014). Hence, the development of the seismic active fault zone west of the well-exposed Al Idrisi and Trougout faults might be attributed to the growth of recent faults owing to westward migration (Vitale et al., 2015) of the deformation during development of the Gibraltar Arc.

The westward migration of the Gibraltar Arc is well constrained by geological (Crespo-Blanc et al., 2016) and GPS data (Fadil et al., 2006; Koulali et al., 2011; Palano et al., 2015). However, the driving mechanism remains a matter of debate, with geodynamic models considering delamination (e.g., Lis Mancilla et al., 2013; Seber et al., 1996) and subduction (e.g., González-Castillo et al., 2015; Gutscher et al., 2012; Pedrera et al., 2011; Ruiz-Constán et al., 2011; Spakman et al., 2018), while rollback is a suitable mechanism for Gibraltar Arc westward displacement and Alboran Sea development. The growth of this seismic NNE-SSW fault zone occurs in the area of weakest and most attenuated continental crust, corresponding to the central Alboran Sea, bounded by the thick continental crust of the Betic and Rif Cordilleras. In this regional setting, the Eurasian-African convergence developed indentation tectonics (Estrada et al., 2018) accommodated by the Al Idrisi fault zone, which now extends to westward areas.

The development of active fault zones has vast implications for seismic hazard. The reactivation of an existing fracture calls for shear stress on the surface to attain the value of the friction and cohesion (Bott, 1959). Immediately previous to the formation of new fractures, shear stress would have to be above the values of friction in addition to cohesion—considerably higher (Anderson, 1951; Hajiabdolmajid et al., 2002). Given the same background setting, the development of a recent fault zone would allow for the accumulation of higher elastic deformation at the fault edges than along a well-developed previous fracture. These factors determine that the propagation of a recent fault, as occurs in the southern Alboran Sea, can produce earthquakes of higher magnitudes than preexisting faults. The highest-magnitude earthquakes of 2004 (d'Acremont et al., 2014; Galindo-Zaldívar et al., 2009) and 2016–2017 occurred in areas of recently developed fault segments with scarce evidence of deformation at the surface (Figure 10). Such faults tend to be particularly active in their initial stage of development, entailing high seismic hazard, and are moreover difficult to detect because of the low amount of accumulated deformation due to their recent age.

5. Conclusions

The Alboran Sea 2016–2017 seismic sequence constitutes a unique opportunity to analyze the development of recent faults in conjunction with seismic hazard. This sequence occurred in the southern part of an active deformation zone crossing the central Alboran Sea and had a main event (M_w = 6.3, 25 January 2016) located along the corner between the NNE-SSW and ENE-WSW deformation alignments, which are 10–20-km wide. The 40-km-long NNE-SSW alignment is located in the Nekor Basin and Francesc Pagès seamount, west of the sea bottom Al Idrisi Fault trace, and the ENE-WSW one is along the northern side of Alboran Ridge and Francesc Pagès seamount. Data recorded during the INCRISIS cruise reveal that the ENE-WSW alignment is mainly characterized by recurrent MTDs that could be linked to earthquake and tectonic activity owing to uplift of the Alboran Ridge and Francesc Pagés antiforms. The NNE-SSW seismicity alignment is related to deep vertical sinistral faults, demonstrated by earthquake focal mechanisms, offset 5 to 10 km westward from the former Al Idrisi Fault. The major NNE-SSW deep sinistral fault zone responsible for the 2016–2017 main events would have activated fault segments up to 15 to 20 km in length for single events. The INCRISIS cruise reveals evidence for recent near-surface ruptures in NW-SE normal faults. These recent faults are related to the western boundary of the deformation zone, bounded eastward by the Al Idrisi Fault; although it is the main fault with seafloor expression, it has segments without recent activity. The present-day stress from earthquake focal mechanisms of 2016–2017 constrains a maximum prolate to triaxial compression inclined toward N319°E in the NNE-SSW alignment, and N332°E in the ENE-WSW alignment, with related orthogonal extension. Stresses are oblique to the N173°E shortening determined by GPS data that support sinistral slip behavior, with some extent of northwestward thrusting.

These data reveal a westward migration and offset of active deformation with respect to the already developed Al Idrisi Fault (Figure 10) that may be linked to the westward development of the Gibraltar Arc. Moreover, the NNE-SSW deformation zone is segmented and was progressively reactivated near the

African coast in the 1993–1994 seismic sequence, the southern onshore part being affected in 2004 and probably activating NNE-SSW sinistral and WNW-ESE dextral faults, with deformation later propagating offshore toward the northeast in 2016–2017. The present-day NW-SE Eurasian-African plate convergence in the westernmost Mediterranean and the inherited heterogeneous rigid basement structures determine the location of deformation areas. At present, a main NNE-SSW sinistral deformation fault zone, including the Al Idrisi Fault and recent developed faults offset to the west, connects the NW-SE extensional faults of the Campo de Dalias's northern edge (Betic Cordillera) with the southern edge's normal splay faults located at the Nekor Basin in the Rif (Figure 10). This setting also contributes to the local crustal thinning of Nekor Basin supported by gravity data.

Geological hazard in the central Alboran Sea is closely related to the seismicity that constitutes a main triggering mechanism of MTDs and is moreover responsible for coseismic seafloor displacements. The development of recent faults that condition the westward widening of the fault zone compared with the already developed faults would imply the activity of the largest segments and the greatest accumulation of elastic energy, producing high-magnitude earthquakes that increase seismic hazard. In any case, low accumulated deformation and recent activity are predominant features making it possible to recognize such faults and therefore deserving further analysis through a multidisciplinary approach.

Acknowledgments

We acknowledge the comments of Prof. N. Niemi, Prof. J. Bruce H. Shyu, Prof. M-A. Gutscher, and three anonymous reviewers, which served to improve the quality of this paper. We also thank A. Mandarieta for his help with the figures. The geological data referenced in this paper are available in the text, the seismicity data are available on the IGN website at http://www.ign.es/web/ign/portal/sis-catalogo-terremotos, and the marine geophysical data are available on the ICM-CSIC website at http://gma.icm.csic.es/sites/default/files/geowebs/OLsurveys/index.htm. This study was supported by the Spanish projects INCRISIS, DAMAGE (CGL2016-80687-R AEI/FEDER) and FAUCES (CTM2015-65461-C2-1-R), RNM 148 - Junta de Andalucía, and Marlboro cruises. French program Actions Marges, the EUROFLEETS program-SARAS cruise (FP7/2007-2013; 228344). The participation of D. Palomino and J. T. Vazquez was funded by the IEO project RIGEL.

References

Akoglu, A. M., Cakir, Z., Meghraoui, M., Belabbes, S., El Alami, S. O., Ergintav, S., & Akyüz, H. S. (2006). The 1994–2004 Al Hoceima (Morocco) earthquake sequence: Conjugate fault ruptures deduced from InSAR. *Earth and Planetary Science Letters*, *252*(3-4), 467–480. https://doi.org/10.1016/j.epsl.2006.10.010

Ammar, A., Mauffret, A., Gorini, C., & Jabour, H. (2007). The tectonic structure of the Alboran Margin of Morocco. *Revista de la Sociedad Geológica de España*, *20*, 247–271.

Anderson, E. M. (1951). *The dynamics of faulting and dyke formation with applications to Britain*. New York: Hafner Pub. Co.

Andrieux, J., Fontbote, J. M., & Mattauer, M. (1971). Sur un modèle explicatif de l'Arc de Gibraltar. *Earth and Planetary Science Letters*, *12*(2), 191–198. https://doi.org/10.1016/0012-821X(71)90077-X

Argus, D. F., Gordon, R. G., Heflin, M. B., Ma, C., Eanes, R. J., Willis, P., et al. (2010). The angular velocities of the plates and the velocity of Earth's centre from space geodesy. *Geophysical Journal International*, *180*(3), 913–960. https://doi.org/10.1111/j.1365-246X.2009.04463.x

Bott, M. H. P. (1959). The mechanics of oblique slip faulting. *Geological Magazine*, *96*(2), 109–117. https://doi.org/10.1017/S0016756800059987

Bourgois, J., Mauffret, A., Ammar, A., & Demnati, A. (1992). Multichannel seismic data imaging of inversion tectonics of the Alboran Ridge (western Mediterranean Sea). *Geo-Marine Letters*, *12*(2-3), 117–122. https://doi.org/10.1007/BF02084921

Buforn, E., Pro, C., Cesca, S., Udias, A., & del Fresno, C. (2011). The 2010 Granada, Spain, deep earthquake. *Bulletin of the Seismological Society of America*, *101*(5), 2418–2430. https://doi.org/10.1785/0120110022

Buforn, E., Pro, C., Sanz de Galdeano, C., Cantavella, J. V., Cesca, S., Caldeira, B., et al. (2017). The 2016 south Alboran earthquake (M_w = 6.4): A reactivation of the Ibero-Maghrebian region? *Tectonophysics*, *712-713*, 704–715. https://doi.org/10.1016/j.tecto.2017.06.033

Buforn, E., Sanz de Galdeano, C., & Udías, A. (1995). Seismotectonics of the Ibero-Maghrebian region. *Tectonophysics*, *248*(3-4), 247–261. https://doi.org/10.1016/0040-1951(94)00276-F

Buforn, E., Udias, A., & Colombas, M. (1988). Seismicity, source mechanisms and tectonics of the Azores-Gibraltar plate boundary. *Tectonophysics*, *152*(1–2), 89–118.

Buforn, E., Udias, A., & Madariaga, R. (1991). Intermediate and deep earthquakes in Spain. In A. Udías & E. Buforn (Eds.), *Source Mechanism and Seismotectonics* (pp. 375–393). Basel: Springer, Birkhäuser. https://doi.org/10.1007/978-3-0348-8654-3_2

Carreño-Herrero, E., & Valero-Zornoza, J. F. (2011). Sismicidad de la Península Ibérica en el periodo instrumental: 1985-2011. *Enseñanza de las Ciencias de la Tierra*, *19*, 289–295.

Casas, A., & Carbó, A. (1990). Deep structure of the Betic Cordillera derived from the interpretation of a complete Bouguer anomaly map. *Journal of Geodynamics Series*, *12*(2-4), 137–147. https://doi.org/10.1016/0264-3707(90)90003-D

Casas, D., Ercilla, G., Yenes, M., Estrada, F., Alonso, B., García, M., & Somoza, L. (2011). The Baraza Slide: Model and dynamics. *Marine Geophysical Researches*, *32*(1-2), 245–256. https://doi.org/10.1007/s11001-011-9132-2

Comas, M., García-Dueñas, V., & Jurado, M. (1992). Neogene tectonic evolution of the Alboran Sea from MCS data. *Geo-Marine Letters*, *12*(2-3), 157–164. https://doi.org/10.1007/BF02084927

Comas, M. C., Platt, J. P., Soto, J. I., & Watts, A. B. (1999). The origin and tectonic history of the Alboran Basin: Insights from Leg 161 results. In R. Zahn, M. C. Comas & A. Klaus (Eds.), *Proceedings of the ocean drilling program scientific results* (Vol. 161, pp. 555–580). College Station, TX: Ocean Drilling Program.

Cowie, P. A., & Scholz, C. H. (1992). Growth of faults by accumulation of seismic slip. *Journal of Geophysical Research*, *97*(B7), 11,085–11,095. https://doi.org/10.1029/92JB00586

Crespo-Blanc, A., Comas, M., & Balanyá, J. C. (2016). Clues for a Tortonian reconstruction of the Gibraltar Arc: Structural pattern, deformation diachronism and block rotations. *Tectonophysics*, *683*, 308–324. https://doi.org/10.1016/j.tecto.2016.05.045

d'Acremont, E., Gutscher, M. A., Rabaute, A., Mercier de Lépinay, B., Lafosse, M., Poort, J., et al. (2014). High-resolution imagery of active faulting offshore Al Hoceima, Northern Morocco. *Tectonophysics*, *632*, 160–166. https://doi.org/10.1016/j.tecto.2014.06.008

El Alami, S. O., Tadili, B. A., Cherkaoui, T. E., Medina, F., Ramdani, M., Brahim, L. A., & Harnafi, M. (1998). The Al Hoceima earthquake of May 26, 1994 and its aftershocks: A seismotectonic study. *Annales de Geophysique*, *41*, 519–537.

El Moudnib, L., Villaseñor, A., Harnafi, M., Gallart, J., Pazos, A., Serrano, I., et al. (2015). Crustal structure of the Betic–Rif system, western Mediterranean, from local earthquake tomography. *Tectonophysics*, *643*, 94–105. https://doi.org/10.1016/j.tecto.2014.12.015

Estrada, F., Galindo-Zaldívar, J., Vázquez, J. T., Ercilla, G., D'Acremont, E., Alonso, B., & Gorini, C. (2018). Tectonic indentation in the central Alboran Sea (westernmost Mediterranean). *Terra Nova*, *30*(1), 24–33. https://doi.org/10.1111/ter.12304

Fadil, A., Vernant, P., McClusky, S., Reilinger, R., Gomez, F., Sari, D. B., et al. (2006). Active tectonics of the western Mediterranean: Geodetic evidence for rollback of a delaminated subcontinental lithospheric slab beneath the Rif Mountains, Morocco. *Geology*, *34*(7), 529–532. https://doi.org/10.1130/G22291.1

Frasca, G., Gueydan, F., & Brun, J. P. (2015). Structural record of Lower Miocene westward motion of the Alboran Domain in the western Betics, Spain. *Tectonophysics*, *657*, 1–20. https://doi.org/10.1016/j.tecto.2015.05.017

Galindo-Zaldívar, J., Azzouz, O., Chalouan, A., Pedrera, A., Ruano, P., Ruiz-Constán, A., et al. (2015). Extensional tectonics, graben development and fault terminations in the eastern Rif (Bokoya–Ras Afraou area). *Tectonophysics*, *663*, 140–149. https://doi.org/10.1016/j.tecto.2015.08.029

Galindo-Zaldívar, J., Borque, M. J., Pedrera, A., Marín-Lechado, C., Gil, A. J., & López-Garrido, A. C. (2013). Deformation behaviour of the low-rate active Balanegra Fault Zone from high-precision levelling (Betic Cordillera, SE Spain). *Journal of Geodynamics*, *71*, 43–51.

Galindo-Zaldívar, J., Chalouan, A., Azzouz, O., Sanz de Galdeano, C., Anahnah, F., Ameza, L., et al. (2009). Are the seismological and geological observations of the Al Hoceima (Morocco, Rif) 2004 earthquake (M = 6.3) contradictory? *Tectonophysics*, *475*(1), 59–67. https://doi.org/10.1016/j.tecto.2008.11.018

Galindo-Zaldívar, J., Gil, A. J., Borque, M. J., González-Lodeiro, F., Jabaloy, A., Marin-Lechado, C., et al. (2003). Active faulting in the internal zones of the central Betic Cordilleras (SE, Spain). *Journal of Geodynamics*, *36*(1), 239–250.

Galindo-Zaldivar, J., Gil, A. J., Sanz de Galdeano, C., Lacy, M. C., García-Armenteros, J. A., Ruano, P., et al. (2015). Active shallow extension in central and eastern Betic Cordillera from CGPS data. *Tectonophysics*, *663*, 290–301. https://doi.org/10.1016/j.tecto.2015.08.035

Galindo-Zaldivar, J., González-Lodeiro, F., Jabaloy, A., Maldonado, A., & Schreider, A. (1998). Models of magnetic and Bouguer gravity anomalies for the deep structure of the central Alboran Sea basin. *Geo-Marine Letters*, *18*(1), 10–18. https://doi.org/10.1007/s003670050046

González-Castillo, L., Galindo-Zaldivar, J., de Lacy, M., Borque, M., Martinez-Moreno, F., García-Armenteros, J., & Gil, A. (2015). Active rollback in the Gibraltar Arc: Evidences from CGPS data in the western Betic Cordillera. *Tectonophysics*, *663*, 310–321. https://doi.org/10.1016/j.tecto.2015.03.010

Grevemeyer, I., Gràcia, E., Villaseñor, A., Leuchters, W., & Watts, A. B. (2015). Seismicity and active tectonics in the Alboran Sea, western Mediterranean: Constraints from an offshore-onshore seismological network and swath bathymetry data. *Journal of Geophysical Research: Solid Earth*, *120*, 8348–8365. https://doi.org/10.1002/2015JB012073

Gutscher, M. A., Dominguez, S., Westbrook, G. K., Le Roy, P., Rosas, F., Duarte, J. C., et al. (2012). The Gibraltar subduction: A decade of new geophysical data. *Tectonophysics*, *574–575*, 72–91. https://doi.org/10.1016/j.tecto.2012.08.038

Hajiabdolmajid, V., Kaiser, P. K., & Martin, C. D. (2002). Modelling brittle failure of rock. *International Journal of Rock Mechanics and Mining Sciences*, *39*(6), 731–741. https://doi.org/10.1016/S1365-1609(02)00051-5

Hatzfeld, D. (1976). Deep-structure of Alboran Sea. *Comptes Rendus Hebdomadaires des Séances de l'Académie des Sciences*, *D283*, 1021–1024.

Hauksson, E., Jones, L. M., Hutton, K., & Eberhart-Phillips, D. (1993). The 1992 Landers earthquake sequence: Seismological observations. *Journal of Geophysical Research: Solid Earth*, *98*(B11), 19,835–19,858. https://doi.org/10.1029/93JB02384

IGN (2016). Informe de la actividad sísmica en el Mar de Alborán 2016. (http://www.ign.es/resources/noticias/Terremoto_Alboran.pdf). Instituto Geográfico Nacional – Red Sísmica Nacional, 1–14.

Juan, C., Ercilla, G., Hernández-Molina, J. F., Estrada, F., Alonso, B., Casas, D., et al. (2016). Seismic evidence of current-controlled sedimentation in the Alboran Sea during the Pliocene and Quaternary: Palaeoceanographic implications. *Marine Geology*, *378*, 292–311. https://doi.org/10.1016/j.margeo.2016.01.006

Kariche, J., Meghraoui, M., Timoulali, Y., Cetin, E., & Toussaint, R. (2018). The Al Hoceima earthquake sequence of 1994, 2004 and 2016: Stress transfer and poroelasticity in the Rif and Alboran Sea region. *Geophysical Journal International*, *212*(1), 42–53.

Koulali, A., Ouazar, D., Tahayt, A., King, R. W., Vernant, P., Reilinger, R. E., et al. (2011). New GPS constraints on active deformation along the Africa–Iberia plate boundary. *Earth and Planetary Science Letters*, *308*(1-2), 211–217. https://doi.org/10.1016/j.epsl.2011.05.048

Lafosse, M., d'Acremont, E., Rabaute, A., Mercier de Lépinay, B., Tahayt, A., Ammar, A., & Gorini, C. (2017). Evidence of Quaternary transtensional tectonics in the Nekor basin (NE Morocco). *Basin Research*, *29*(4), 470–489. https://doi.org/10.1111/bre.12185

Larouzière, F., Bolze, J., Bordet, P., Hernandez, J., Montenat, C., & Ott d'Estevou, P. (1988). The Betic segment of the lithospheric Trans-Alboran shear zone during the Late Miocene. *Tectonophysics*, *152*(1-2), 41–52. https://doi.org/10.1016/0040-1951(88)90028-5

Lis Mancilla, F. D., Stich, D., Berrocoso, M., Martín, R., Morales, J., Fernandez-Ros, A., et al. (2013). Delamination in the Betic Range: Deep structure, seismicity, and GPS motion. *Geology*, *41*(3), 307–310.

Locat, J., & Lee, H. J. (2002). Submarine landslides: Advances and challenges. *Canadian Geotechnical Journal*, *39*(1), 193–212. https://doi.org/10.1139/t01-089

López-Casado, C., Sanz de Galdeano, C., Palacios, S. M., & Romero, J. H. (2001). The structure of the Alboran Sea: An interpretation from seismological and geological data. *Tectonophysics*, *338*(2), 79–95. https://doi.org/10.1016/S0040-1951(01)00059-2

Marín-Lechado, C., Galindo-Zaldívar, J., Gil, A. J., Borque, M. J., De Lacy, M. C., Pedrera, A., et al. (2010). Levelling profiles and a GPS network to monitor the active folding and faulting deformation in the Campo de Dalias (Betic Cordillera, southeastern Spain). *Sensors*, *10*(4), 3504–3518. https://doi.org/10.3390/s100403504

Marín-Lechado, C., Galindo-Zaldívar, J., Rodríguez-Fernández, L. R., Serrano, I., & Pedrera, A. (2005). Active faults, seismicity and stresses in an internal boundary of a tectonic arc (Campo de Dalías and Níjar, southeastern Betic Cordilleras, Spain). *Tectonophysics*, *396*(1-2), 81–96. https://doi.org/10.1016/j.tecto.2004.11.001

Martínez-García, P., Comas, M., Lonergan, L., & Watts, A. B. (2017). From extension to shortening: Tectonic inversion distributed in time and space in the Alboran Sea, western Mediterranean. *Tectonics*, *36*, 2777–2805. https://doi.org/10.1002/2017TC004489

Martínez-García, P., Comas, M., Soto, J. I., Lonergan, L., & Watts, A. (2013). Strike-slip tectonics and basin inversion in the western Mediterranean: The post-Messinian evolution of the Alboran Sea. *Basin Research*, *25*(4), 361–387. https://doi.org/10.1111/bre.12005

Martínez-García, P., Soto, J. I., & Comas, M. (2011). Recent structures in the Alboran Ridge and Yusuf fault zones based on swath bathymetry and sub-bottom profiling: Evidence of active tectonics. *Geo-Marine Letters*, *31*(1), 19–36. https://doi.org/10.1007/s00367-010-0212-0

Medina, F., & Cherkaoui, T. E. (2017). The south-western Alboran earthquake sequence of January-March 2016 and its associated coulomb stress changes. *Open Journal of Earthquake Research*, *6*(1), 35–54. https://doi.org/10.4236/ojer.2017.61002

Meissner, R., & Strehlau, J. (1982). Limits of stresses in continental crusts and their relation to the depth-frequency distribution of shallow earthquakes. *Tectonics*, *1*(1), 73–89. https://doi.org/10.1029/TC001i001p00073

De Mets, C., Laffaldano, G., & Merkouriev, S. (2015). High-resolution Neogene and Quaternary estimates of Nubia-Eurasia-North America plate motion. *Geophysical Journal International*, *203*(1), 416–427. https://doi.org/10.1093/gji/ggv277

Michael, A. J. (1984). Determination of stress from slip data: Faults and folds. *Journal of Geophysical Research: Solid Earth*, *89*(B13), 11,517–11,526. https://doi.org/10.1029/JB089iB13p11517

Michelini, A., & Lomax, A. (2004). The effect of velocity structure errors on double-difference earthquake location. *Geophysical Research Letters*, *31*, L09602. https://doi.org/10.1029/2004GL019682

Morales, J., Serrano, I., Jabaloy, A., Galindo-Zaldivar, J., Zhao, D., Torcal, F., & González-Lodeiro, F. (1999). Active continental subduction beneath the Betic Cordillera and the Alboran Sea. *Geology*, *27*(8), 735–738. https://doi.org/10.1130/0091-7613(1999)027<0735:ACSBTB>2.3.CO;2

Palano, M., González, P. J., & Fernández, J. (2015). The diffuse plate boundary of Nubia and Iberia in the western Mediterranean: Crustal deformation evidence for viscous coupling and fragmented lithosphere. *Earth and Planetary Science Letters*, *430*, 439–447. https://doi.org/10.1016/j.epsl.2015.08.040

Pedrera, A., Ruiz-Constán, A., Galindo-Zaldívar, J., Chalouan, A., Sanz de Galdeano, C., Marín-Lechado, C., et al. (2011). Is there an active subduction beneath the Gibraltar orogenic arc? Constraints from Pliocene to present-day stress field. *Journal of Geodynamics*, *52*(2), 83–96 . https://doi.org/10.1016/j.jog.2010.12.003

Poujol, A., Ritz, J. F., Tahayt, A., Vernant, P., Condomines, M., Blard, P. H., et al. (2014). Active tectonics of the Northern Rif (Morocco) from geomorphic and geochronological data. *Journal of Geodynamics*, *77*, 70–88. https://doi.org/10.1016/j.jog.2014.01.004

Ruiz-Constán, A., Galindo-Zaldívar, J., Pedrera, A., Celerier, B., & Marín-Lechado, C. (2011). Stress distribution at the transition from subduction to continental collision (northwestern and central Betic Cordillera). *Geochemistry, Geophysics, Geosystems*, *12*, Q12002. https://doi.org/10.1029/2011GC003824

Sandwell, D. T., Müller, R. D., Smith, W. H., Garcia, E., & Francis, R. (2014). New global marine gravity model from CryoSat-2 and Jason-1 reveals buried tectonic structure. *Science*, *346*(6205), 65–67. https://doi.org/10.1126/science.1258213

Scholz, C. H. (2002). *The mechanics of earthquakes and faulting*. Cambridge, UK: Cambridge University Press. https://doi.org/10.1017/CBO9780511818516

Seber, D., Barazangi, M., Ibenbrahim, A., & Demnati, A. (1996). Geophysical evidence for lithospheric delamination beneath the Alboran Sea and Rif–Betic mountains. *Nature*, *379*(6568), 785–790.

Sibson, R. (1977). Fault rocks and fault mechanisms. *Journal of the Geological Society*, *133*(3), 191–213. https://doi.org/10.1144/gsjgs.133.3.0191

Spakman, W., Chertova, M. V., van den Berg, A., & van Hinsbergen, D. J. J. (2018). Puzzling features of western Mediterranean tectonics explained by slab dragging. *Nature Geoscience*, *11*(3), 211–216. https://doi.org/10.1038/s41561-018-0066-z

Stich, D., Martín, R., & Morales, J. (2010). Moment tensor inversion for Iberia–Maghreb earthquakes 2005–2008. *Tectonophysics*, *483*(3-4), 390–398. https://doi.org/10.1016/j.tecto.2009.11.006

Stich, D., Serpelloni, E., de Lis Mancilla, F., & Morales, J. (2006). Kinematics of the Iberia–Maghreb plate contact from seismic moment tensors and GPS observations. *Tectonophysics*, *426*(3-4), 295–317. https://doi.org/10.1016/j.tecto.2006.08.004

Van der Woerd, J., Dorbath, C., Ousadou, F., Dorbath, L., Delouis, B., Jacques, E., et al. (2014). The Al Hoceima M_w 6.4 earthquake of 24 February 2004 and its aftershocks sequence. *Journal of Geodynamics*, *77*, 89–109. https://doi.org/10.1016/j.jog.2013.12.004

Vavryčuk, V. (2014). Iterative joint inversion for stress and fault orientations from focal mechanisms. *Geophysical Journal International*, *199*(1), 69–77. https://doi.org/10.1093/gji/ggu224

De Vicente, G., Cloetingh, S., Muñoz-Martín, A., Olaiz, A., Stich, D., Vegas, R., et al. (2008). Inversion of moment tensor focal mechanisms for active stresses around the microcontinent Iberia: Tectonic implications. *Tectonics*, *27*, TC1009. https://doi.org/10.1029/2006TC002093

Vitale, S., Zaghloul, M. N., El Ouaragli, B., Tramparulo, F. D. A., & Ciarcia, S. (2015). Polyphase deformation of the Dorsale Calcaire complex and the Maghrebian Flysch Basin units in the Jebha area (Central Rif, Morocco): New insights into the Miocene tectonic evolution of the Central Rif belt. *Journal of Geodynamics*, *90*, 14–31. https://doi.org/10.1016/j.jog.2015.07.002

Watterson, J. (1986). Fault dimensions, displacements and growth. *Pure and Applied Geophysics*, *124*(1-2), 365–373. https://doi.org/10.1007/BF00875732

Wells, D. L., & Coppersmith, K. J. (1994). New empirical relationships among magnitude, rupture length, rupture width, rupture area, and surface displacement. *Bulletin of the Seismological Society of America*, *84*, 974–1002.